

On an exact solution of the Thomas-Fermi equation for a trapped Bose-Einstein condensate with dipole-dipole interactions

Claudia Eberlein,¹ Stefano Giovanazzi,² and Duncan H J O'Dell¹

¹Dept of Physics & Astronomy, University of Sussex, Falmer, Brighton BN1 9QH, England

²School of Physics & Astronomy, University of St Andrews, North Haugh, St Andrews KY16 9SS, Scotland

(Dated: January 23, 2020)

We derive an exact solution to the Thomas-Fermi equation for a Bose-Einstein condensate which has dipole-dipole interactions as well as the usual *s*-wave contact interaction, in a harmonic trap. Remarkably, despite the non-local anisotropic nature of the dipolar interaction the solution is an inverted parabola, as in the pure *s*-wave case, but with a different aspect ratio. Various properties such as electrostriction and stability are discussed.

PACS numbers: 03.75.Kk, 34.20.Cf, 32.80.Qk, 75.80.+q

I. INTRODUCTION

Usually, the dominant interatomic interactions in an atomic Bose-Einstein condensate (BEC) [1, 2] are of the van der Waals (vdW) type, which falls off as r^{-6} , and is short-range in comparison to the de Broglie wavelength of the atoms. The vdW interactions can be most conveniently incorporated into a mean-field description of the condensate via a delta-function pseudo-potential

$$U(\mathbf{r}) = 4\pi\hbar^2 a_s \delta(\mathbf{r})/m \equiv g\delta(\mathbf{r}) \quad (1)$$

involving just the *s*-wave scattering length a_s and atomic mass m . The interactions then appear as a cubic non-linearity in the Gross-Pitaevskii equation [3] for the order parameter $\psi(\mathbf{r})$ of a trapped zero-temperature BEC

$$\mu\psi(\mathbf{r}) = \left\{ -\frac{\hbar^2}{2m} \nabla^2 + V_{\text{trap}}(\mathbf{r}) + g|\psi(\mathbf{r})|^2 \right\} \psi(\mathbf{r}) \quad (2)$$

where μ is the chemical potential. The trapping potential, V_{trap} , due to a magnetic or optical trap is typically harmonic, $V_{\text{trap}} = (m/2)[\omega_x^2 x^2 + \omega_y^2 y^2 + \omega_z^2 z^2]$.

The Thomas-Fermi regime for a trapped Bose-Einstein condensate (BEC) is reached when the zero-point kinetic energy is vanishingly small in comparison to both the potential energy due to the trap and the interaction energy between atoms [2]. Many of the current atomic BEC experiments [1] satisfy these conditions, which tend to hold for condensates containing a large number of atoms. When the kinetic energy is neglected the time-independent Gross-Pitaevskii equation (2) can be trivially solved for the static condensate density,

$$n(\mathbf{r}) \equiv |\psi(\mathbf{r})|^2 = [\mu - V_{\text{trap}}(\mathbf{r})]/g \quad \text{for } n(\mathbf{r}) \geq 0, \quad (3)$$

and $n(\mathbf{r}) = 0$ elsewhere. Thus the density profile is completely determined by the trapping potential, and in a harmonic trap $n(\mathbf{r})$ has an (inverted) parabolic profile and the same aspect ratio as the trap.

Our aim here is to obtain similar exact results for a BEC in which dipole-dipole interactions play an important role. Compared to the vdW interaction the dipolar interaction is long-range and anisotropic, and consequently these systems can be expected to exhibit novel

behaviour including unusual stability properties [4, 5, 6], exotic ground states such as supersolid [7, 8] and checkerboard phases [8], and modified excitation spectra [9, 10], even to the extent of a roton minimum [11, 12] in the dispersion relation. We have recently investigated the exact dynamics of a dipolar BEC in the Thomas-Fermi limit [13], including the quadrupole and monopole shape oscillation frequencies. Here we concentrate on the static properties of the dipolar BEC, such as stability and electrostriction (change in volume due to an applied electric field), and give a full derivation of the static solution which was only stated in [13]. We also calculate the dipole-dipole potential outside the boundary of the condensate, which has a bearing on the stability of a dipolar BEC, but also on a lattice array of dipolar BECs, the effective giant dipole on each site being coupled to its neighbors by dipole-dipole interactions [14].

The long-range part of the interaction between two dipoles separated by \mathbf{r} , and aligned by an external field along a unit vector $\hat{\mathbf{e}}$, is given by

$$U_{\text{dd}}(\mathbf{r}) = \frac{C_{\text{dd}}}{4\pi} \hat{\mathbf{e}}_i \hat{\mathbf{e}}_j \frac{(\delta_{ij} - 3\hat{r}_i \hat{r}_j)}{r^3} \quad (4)$$

where the coupling $C_{\text{dd}}/(4\pi)$ depends on the specific realization. Marinescu and You [15] investigated the low-energy scattering of two atoms with dipole-dipole interactions induced by a static electric field, $\mathbf{E} = E\hat{\mathbf{e}}$, so that $C_{\text{dd}} = E^2 \alpha^2 / \epsilon_0$. Yi and You [16] then went on to consider a BEC composed of such atoms. Another possible scenario is permanent magnetic dipoles, d_m , aligned by an external magnetic field, $\mathbf{B} = B\hat{\mathbf{e}}$, leading to a coupling $C_{\text{dd}} = \mu_0 d_m^2$. A BEC with magnetic dipole-dipole interactions was first discussed by Góral, Rzżewski, and Pfau [4]. A measure of the strength of the long-range dipole-dipole interaction relative to the *s*-wave scattering energy is provided by the dimensionless quantity

$$\varepsilon_{\text{dd}} \equiv \frac{C_{\text{dd}}}{3g}. \quad (5)$$

This definition arises naturally from an analysis of the frequencies of collective excitations (Bogoliubov spectrum) in a *homogeneous* dipolar BEC [4, 17]. As we shall

see later on, the BEC is stable as long as $0 \leq \varepsilon_{dd} < 1$, but becomes either only metastable or absolutely unstable when $\varepsilon_{dd} > 1$. Note that in the presence of a strong electric field the *s*-wave scattering length can be modified [9, 15], and therefore g and hence ε_{dd} should be treated as effective quantities when dealing with electrically induced dipoles.

Although the magnetic interaction between two atoms is often masked by a stronger *s*-wave interaction, two recent proposals indicate how magnetic dipolar effects can be enhanced, either by rotating the magnetic field in resonance with a collective excitation frequency of the system [17], or by using a Feshbach resonance to reduce the *s*-wave scattering length [18]. Other suggestions to realize BECs with strong dipolar interactions include polar molecules [4] and Rydberg atoms [5]. We have previously also discussed laser induced (dynamic) dipole-dipole interactions which differ from the static case of Eq. (4) by extra retarded terms, including an r^{-1} term which is always attractive [19]. In certain situations this very long-range part of the interaction is important and can be responsible for unique features such as self-binding, and plasmon-like collective excitations. Here, however, we confine ourselves to the static case, which could be realized by static fields but also by using a laser provided the atomic separation is considerably smaller than the laser wavelength.

II. THOMAS-FERMI EQUATION FOR A DIPOLEAR BEC

Defining the Thomas-Fermi equation for a BEC as being the time-independent Gross-Pitaevskii equation without the kinetic energy term, we seek an exact solution for the density, $n(\mathbf{r})$, of a condensate with both dipole-dipole interactions and the usual short-range *s*-wave scattering in a harmonic trap, which for simplicity (though not necessity) we take to be cylindrically symmetric ($\omega_x = \omega_y$). The Thomas-Fermi equation then reads

$$\mu = \frac{1}{2}m(\omega_x^2\rho^2 + \omega_z^2z^2) + gn(\mathbf{r}) + \Phi_{dd}(\mathbf{r}) \quad (6)$$

where $\rho^2 = x^2 + y^2$, and $\Phi_{dd}(\mathbf{r})$ is the mean-field potential due to dipole-dipole interactions

$$\Phi_{dd}(\mathbf{r}) \equiv \int d^3r' U_{dd}(\mathbf{r} - \mathbf{r}')n(\mathbf{r}') \quad (7)$$

The intuitive form of Eqns (6) and (7) has been verified by Yi and You [9] on the basis of a calculation of the two-body T-matrix.

The presence of the non-local dipolar mean-field potential $\Phi_{dd}(\mathbf{r})$ means that the Thomas-Fermi Eq. (6) is an integral equation and so less trivial to solve than in the purely local delta-function pseudo-potential case. However, it is straightforward to demonstrate that this equation also admits an inverted-parabola as a self-consistent

solution. We begin our analysis with a suggestive re-casting of the dipole-dipole term using the mathematical identity

$$\frac{(\delta_{ij} - 3\hat{r}_i\hat{r}_j)}{r^3} = -\nabla_i\nabla_j \frac{1}{r} - \frac{4\pi}{3}\delta_{ij}\delta(\mathbf{r}) \quad (8)$$

We can then write

$$\Phi_{dd}(\mathbf{r}) = -C_{dd}\hat{e}_i\hat{e}_j \left(\nabla_i\nabla_j\phi(\mathbf{r}) + \frac{\delta_{ij}}{3}n(\mathbf{r}) \right) \quad (9)$$

$$\text{with } \phi(\mathbf{r}) \equiv \frac{1}{4\pi} \int \frac{d^3r' n(\mathbf{r}')}{|\mathbf{r} - \mathbf{r}'|} \quad (10)$$

The problem thereby reduces to an analogy with electrostatics, and we need only calculate the ‘potential’ $\phi(\mathbf{r})$ arising from the ‘static charge’ distribution $n(\mathbf{r})$. In particular, $\phi(\mathbf{r})$ given by (10) must obey Poisson’s equation $\nabla^2\phi = -n(\mathbf{r})$. Adopting the following inverted-parabola as an ansatz for the density profile of an N -atom condensate

$$n(\mathbf{r}) = n_0 \left[1 - \frac{\rho^2}{R_x^2} - \frac{z^2}{R_z^2} \right] \quad \text{for } n(\mathbf{r}) \geq 0 \quad (11)$$

with radii $R_x = R_y$ and R_z , and where the central density n_0 is constrained by normalization to be

$$n_0 = 15N/(8\pi R_x^2 R_z) \quad (12)$$

then Poisson’s equation will be satisfied by an ‘electrostatic potential’ of the general form

$$\phi(\mathbf{r}) = a_0 + a_1\rho^2 + a_2z^2 + a_3\rho^4 + a_4z^4 + a_5\rho^2z^2 \quad (13)$$

However, by Eq. (9), the physical dipolar contribution $\Phi_{dd}(\mathbf{r})$ to the mean-field potential inside the inverted-parabola BEC (11) will now itself also be *parabolic*, just like the potentials due to the harmonic trap and the local *s*-wave scattering interaction. Thus the Thomas-Fermi equation (6) contains only parabolic and constant terms and so, remarkably, just as in the pure *s*-wave case, in the presence of dipole-dipole interactions a parabolic density profile is also an exact solution of the Thomas-Fermi problem in a harmonic trap, although this time we should expect that the condensate aspect ratio differs from that of the trap. It remains to determine the coefficients appearing in (13) and in (11) and adjust them in such a way that the Thomas-Fermi equation is satisfied. To this end we shall evaluate the integral (10) for a density of the form (11). This is an arduous task because the domain of integration is bounded by and has the symmetry of a spheroid or, in the general case, even of an ellipsoid. Calculating the integral is possible only if one takes explicit account of this symmetry, and we shall demonstrate two independent ways of doing that. One is to transform into spheroidal coordinates, use the known Green’s function of Poisson’s equation in these coordinates [20], and subsequently transform back into Cartesian coordinates. The other is to start from basics and integrate over successive

thin ellipsoidal shells. While the former approach is also quite involved it is simpler than the latter. However, if we were to drop our simplifying assumption of cylindrical symmetry, the second approach is the only workable as the general solution of Poisson's equation in general ellipsoidal coordinates is unmanageably complicated because the separation constants do not separate in these coordinates [20, p. 757]. The second approach is presented in appendix A.

III. GREEN'S FUNCTION IN SPHEROIDAL COORDINATES

We now demonstrate the Green's function approach. For prolate spheroidal coordinates (ξ, η, φ) we have $x = q\sqrt{(\xi^2 - 1)(1 - \eta^2)} \cos \varphi$, $y = q\sqrt{(\xi^2 - 1)(1 - \eta^2)} \sin \varphi$, $z = q\xi\eta$. Surfaces of constant ξ are confocal spheroids whose eccentricity is $1/\xi$, and ξ runs between 1 and ∞ . Surfaces of constant η are confocal two-sheet hyperboloids of revolution, and η runs between -1 and 1. For $R_z > R_x$ the boundary of the density profile (11) is a prolate (cigar-like) spheroid with semimajor axis R_z , semiminor axis R_x , and eccentricity $\sqrt{1 - R_x^2/R_z^2}$. To make the spheroidal coordinate system confocal to that boundary we need to choose the scaling constant $q = \sqrt{R_z^2 - R_x^2}$. Then we can use the Green's function in prolate spheroidal coordinates [20] to write the potential (10) as

$$\begin{aligned} \phi(\xi, \eta, \varphi) = & \frac{R_z^2 - R_x^2}{2} \left[\int_1^\xi d\xi' \int_{-1}^1 d\eta' (\xi'^2 - \eta'^2) n(\xi', \eta') \right. \\ & \times \sum_{\ell=0}^{\infty} (2\ell + 1) P_\ell(\eta) P_\ell(\eta') Q_\ell(\xi) P_\ell(\xi') \\ & + \int_\xi^{1/\sqrt{1 - R_x^2/R_z^2}} d\xi' \int_{-1}^1 d\eta' (\xi'^2 - \eta'^2) n(\xi', \eta') \\ & \left. \times \sum_{\ell=0}^{\infty} (2\ell + 1) P_\ell(\eta) P_\ell(\eta') P_\ell(\xi) Q_\ell(\xi') \right], \end{aligned}$$

where P_ℓ are Legendre functions of the first and Q_ℓ of the second kind. Since $n(\mathbf{r})$ is quadratic in x , y , and z it is quadratic in ξ and η , and all integrals in the above expression are elementary. Performing the η' integration first we see that the only contributing ℓ are 0, 2, and 4. To re-express the result for $\phi(\xi, \eta, \varphi)$ in Cartesian coordinates we need to make the substitutions $\xi = (r_1 + r_2)/(2q)$ and $\eta = (r_1 - r_2)/(2q)$ with $r_1 = [x^2 + y^2 + (z + q)^2]^{1/2}$ and $r_2 = [x^2 + y^2 + (z - q)^2]^{1/2}$. We thereby

obtain a 'potential' of the form predicted by Eq. (13):

$$\begin{aligned} \phi(\mathbf{r}) = & \frac{n_0 R_x^2}{192(1 - \kappa^2)^2} \{ 24\Xi(1 - \kappa^2)^2 \\ & + 48(1 - \kappa^2)(2 - \Xi)(z/R_z)^2 \\ & - 24(1 - \kappa^2)(2 - \kappa^2\Xi)(\rho/R_x)^2 \\ & + 8(2\kappa^2 - 8 + 3\Xi)(z/R_z)^4 \\ & + 3[2(2 - 5\kappa^2) + 3\kappa^4\Xi](\rho/R_x)^4 \\ & + 24(2 + 4\kappa^2 - 3\kappa^2\Xi)(\rho/R_x)^2(z/R_z)^2 \} \end{aligned} \quad (14)$$

where $\kappa \equiv R_x/R_z$ is the aspect ratio of the BEC and

$$\Xi \equiv \frac{1}{\sqrt{1 - \kappa^2}} \ln \frac{1 + \sqrt{1 - \kappa^2}}{1 - \sqrt{1 - \kappa^2}} \quad \text{for } \kappa < 1 \quad (\text{prolate}). \quad (15)$$

If $R_x > R_z$ then the boundary of the density profile (11) is an oblate (pancake-like) spheroid, and we have to use oblate spheroidal coordinates $x = q\sqrt{(\xi^2 + 1)(1 - \eta^2)} \cos \varphi$, $y = q\sqrt{(\xi^2 + 1)(1 - \eta^2)} \sin \varphi$, $z = q\xi\eta$. Surfaces of constant ξ are again confocal spheroids but now with eccentricity $1/\sqrt{\xi + 1}$, and ξ running between 0 and ∞ . We have to choose $q = \sqrt{R_x^2 - R_z^2}$ to make the coordinate system confocal to the boundary of $n(\mathbf{r})$. Using the Green's function in oblate spheroidal coordinates [20, 21] we find for the potential

$$\begin{aligned} \phi(\xi, \eta, \varphi) = & \frac{R_x^2 - R_z^2}{2} \left[\int_0^\xi d\xi' \int_{-1}^1 d\eta' (\xi'^2 + \eta'^2) n(\xi', \eta') \right. \\ & \times i \sum_{\ell=0}^{\infty} (2\ell + 1) P_\ell(\eta) P_\ell(\eta') Q_\ell(i\xi) P_\ell(i\xi') \\ & + \int_\xi^{1/\sqrt{R_x^2/R_z^2 - 1}} d\xi' \int_{-1}^1 d\eta' (\xi'^2 + \eta'^2) n(\xi', \eta') \\ & \left. \times i \sum_{\ell=0}^{\infty} (2\ell + 1) P_\ell(\eta) P_\ell(\eta') P_\ell(i\xi) Q_\ell(i\xi') \right]. \end{aligned}$$

To return to Cartesian coordinates we need to make the substitutions $\xi = (\sqrt{x^2 + y^2 + (z + iq)^2} + \sqrt{x^2 + y^2 + (z - iq)^2})/(2q)$ and $\eta = (\sqrt{x^2 + y^2 + (z + iq)^2} - \sqrt{x^2 + y^2 + (z - iq)^2})/(2iq)$. Then we find that the result for the potential is the same as in Eq. (14) but with

$$\Xi \equiv \frac{2}{\sqrt{\kappa^2 - 1}} \arctan \sqrt{\kappa^2 - 1} \quad \text{for } \kappa > 1 \quad (\text{oblate}). \quad (16)$$

The prolate and oblate cases are of course connected by analytic continuation, which however cannot be used to determine one from the other because of the ambiguity of sheets in the complex plane.

In order to simplify the expressions that will follow, and in order to conform with existing notation in the literature [9, 22], rather than working with the function $\Xi(\kappa)$, we shall work instead with $f(\kappa)$:

$$f(\kappa) \equiv \frac{2 + \kappa^2[4 - 3\Xi(\kappa)]}{2(1 - \kappa^2)}. \quad (17)$$

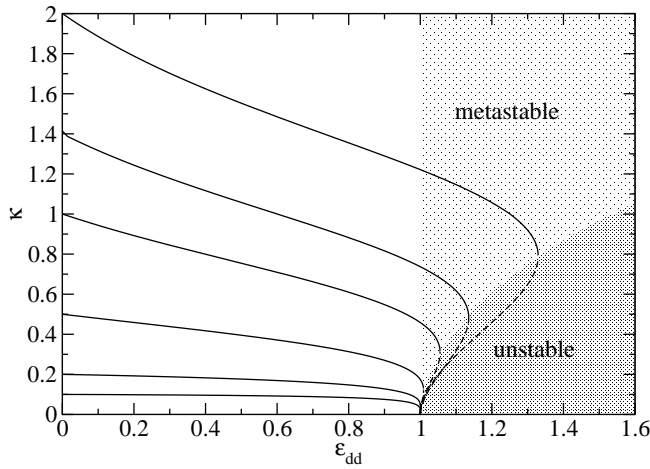


FIG. 1: Aspect ratio of the condensate as a function of the dipole-dipole to s -wave coupling ratio ε_{dd} . Each line is for a different trap aspect ratio γ , which can be read off by noting that $\kappa(\varepsilon_{dd} = 0) = \gamma$. When $0 < \kappa < 1$ the condensate is prolate, for $\kappa > 1$ it is oblate. Likewise, when $0 < \gamma < 1$ the trap is prolate, and when $\gamma > 1$ the trap is oblate. Dashed lines indicate unstable branches.

$f(\kappa)$ is a monotonically decreasing function of κ , having values in the range $1 \geq f(\kappa) \geq -2$, passing through zero at $\kappa = 1$.

IV. SOLUTION OF THE THOMAS-FERMI EQUATION

In this paper we shall take the external field to be along the z -axis. Then the result (14) for the ‘electrostatic potential’ $\phi(\mathbf{r})$ yields, by virtue of Eq. (9), a parabolic dipolar potential

$$\Phi_{dd} = \frac{n_0 C_{dd}}{3} \left[\frac{\rho^2}{R_x^2} - \frac{2z^2}{R_z^2} - f(\kappa) \left(1 - \frac{3}{2} \frac{\rho^2 - 2z^2}{R_x^2 - R_z^2} \right) \right] \quad (18)$$

which is valid inside the condensate (the potential outside the condensate boundary will be discussed in section V). Substituting $\Phi_{dd}(\mathbf{r})$ into the Thomas-Fermi Eq. (6) and comparing the coefficients of ρ^2 , z^2 , and 1, yields three coupled equations. The first equation, due to the constant terms, gives the chemical potential

$$\mu = gn_0 [1 - \varepsilon_{dd} f(\kappa)]. \quad (19)$$

This equation indicates that, all other things being equal, the effect of dipole-dipole interactions is to lower the chemical potential (which is proportional to the mean-field energy per particle) of a prolate ($\kappa < 1$) condensate, whilst raising that of an oblate ($\kappa > 1$) condensate. The radii $R_x (= R_y)$ and R_z of the exact parabolic solution (11) are obtained from the coefficients of ρ^2 and z^2 . We find

$$R_x = R_y = \left[\frac{15gN\kappa}{4\pi m\omega_x^2} \left\{ 1 + \varepsilon_{dd} \left(\frac{3}{2} \frac{\kappa^2 f(\kappa)}{1 - \kappa^2} - 1 \right) \right\} \right]^{1/5} \quad (20)$$

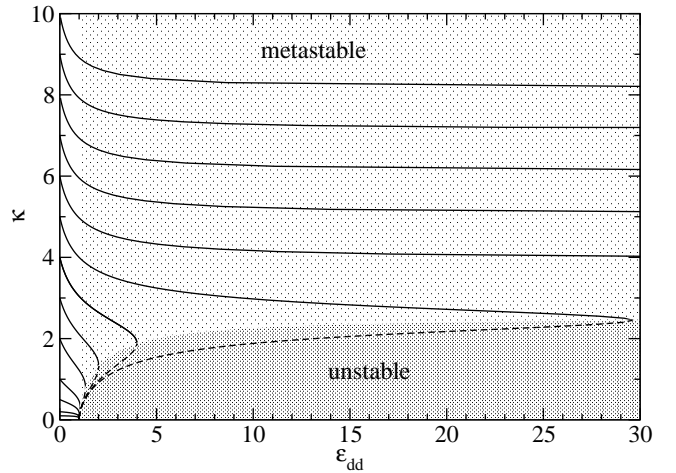


FIG. 2: Aspect ratio of the condensate as a function of ε_{dd} . This is an expanded version of Fig. 1, illustrating the surprising result that beyond a certain critical oblateness of the trap ($\gamma > \gamma_{crit} = 5.1701$) the system is metastable to scaling deformations, even for arbitrarily high values of the dipolar interaction strength. At the boundary value $\gamma = \gamma_{crit}$, one finds $\kappa \rightarrow 2.5501$ for $\varepsilon_{dd} \rightarrow \infty$.

and $R_z = R_x/\kappa$. The aspect ratio κ is determined by solving a transcendental equation

$$3\kappa^2\varepsilon_{dd} \left[\left(\frac{\gamma^2}{2} + 1 \right) \frac{f(\kappa)}{1 - \kappa^2} - 1 \right] + (\varepsilon_{dd} - 1) (\kappa^2 - \gamma^2) = 0 \quad (21)$$

where $\gamma = \omega_z/\omega_x$ is the ratio of the harmonic trapping frequencies. In fact, a property such as the aspect ratio is insensitive to the details of the density profile and Eq. (21) has been obtained previously using a Gaussian variational ansatz for the density [9, 22]. Figures 1 and 2 show examples of the dependence of κ upon ε_{dd} for oblate, spherical and prolate traps. The effect of dipole-dipole forces polarized along the z -axis is to make the condensate more cigar-shaped along z . For an oblate trap ($\gamma > 1$) the BEC becomes exactly spherical when $\varepsilon_{dd} = (5/2)(\gamma^2 - 1)/(\gamma^2 + 2)$.

In order to illustrate the static properties of the Thomas-Fermi solution for a dipolar BEC we imagine an experiment with a large fixed number of atoms, N , in a trap set to a particular aspect ratio, γ , where the value of ε_{dd} is adiabatically increased from zero. For electrically induced dipoles this would involve increasing the electric field, whereas for magnetic dipoles one could either rotate the external magnetic field, gradually changing the angle of rotation [17], or reduce the s -wave scattering length using a Feshbach resonance. The system then follows one of the curves shown in Figures 1 and 2. In the absence of the external field, when $\varepsilon_{dd} = 0$, the condensate aspect ratio matches that of the trap, $\kappa = \gamma$. When the dipole-dipole interactions are switched on the condensate becomes more prolate than the trap and one always has $\kappa < \gamma$. As long as $0 \leq \varepsilon_{dd} < 1$, the transcendental equation (21) has a single solution, κ , for any choice of trap, γ . The behavior for $\varepsilon_{dd} > 1$ is more complicated and re-

quires an analysis of the stability properties of a dipolar BEC, which we give in the next section.

V. STABILITY OF A DIPOLAR BEC

The partially attractive nature of the dipole-dipole interaction (4) has been widely predicted [4, 5, 6, 9] to lead to a collapse of the BEC when the dipolar interaction strength exceeds a certain critical value, $\varepsilon_{dd}^{\text{crit}}$. In the Thomas-Fermi limit $\varepsilon_{dd}^{\text{crit}}$ depends only upon the trap aspect ratio γ . Both the parabolic solution presented here and the Gaussian variational ansatz indicate that above $\varepsilon_{dd}^{\text{crit}}$ the system is liable to collapse towards an infinitely thin and long prolate ‘pencil’ oriented along the field polarization direction i.e. $\kappa \rightarrow 0$, since the system lowers its energy by arranging the dipoles end-to-end. However, in reality a transition to another (more structured?) state (see [4, 7, 8, 11, 12]) presumably occurs before the system becomes truly singular. Bearing this in mind we shall consider below three nominally different types of instability: local density perturbations, ‘scaling’ deformations, and the ‘Saturn-ring’ instability. The latter occurs due to a peculiarity in the potential that would be seen by an atom located *outside* the boundary of the BEC, and may result in a previously unforeseen type of instability. All of them predict the onset of instability when $\varepsilon_{dd} \geq 1$. Nevertheless, we have included in the figures values of ε_{dd} exceeding unity, our justification being partly mathematical curiosity, and partly because the inclusion of kinetic energy would extend the stability of a dipolar BEC beyond that of the strict Thomas-Fermi limit considered here.

A. Local density perturbations

In a homogeneous dipolar BEC phonons are known to cause instabilities when $\varepsilon_{dd} > 1$, as can be seen directly from the Bogoliubov dispersion relation, which becomes imaginary when $\varepsilon_{dd} > 1$ [4, 17]. Here, we should expect an analogous instability due to local density perturbations having a wavelength much smaller than the dimensions of the condensate. For example, Santos *et al* [12] recently showed that an infinite-pancake dipolar BEC, homogenous in two directions and parabolic in the third, is unstable when $\varepsilon_{dd} > 1$ for a density exceeding a critical value.

B. Scaling deformations

We use the term ‘scaling’ deformation to describe perturbations that merely re-scale the parabolic solution (11), i.e. that change $R_x = R_y$ and R_z from their equilibrium values (20), but leave the basic form of the parabolic solution the same. Since the equilibrium values of the radii are determined by the transcendental equation (21),

which also occurs in the context of a Gaussian variational solution, much of what we shall say below has already been described by other authors, including Santos *et al* [5], and Yi and You [9].

Information on the stability of the parabolic solution can be gained from analyzing the behavior of the energy functional $E_{\text{tot}} = E_{\text{trap}} + E_{s\text{-wave}} + E_{dd}$ evaluated over a general parabolic density profile (11)

$$E_{\text{tot}} = \frac{N}{14} m \omega_x^2 R_x^2 \left(2 + \frac{\gamma^2}{\kappa^2} \right) + \frac{15}{28\pi} \frac{N^2 g}{R_x^2 R_z} [1 - \varepsilon_{dd} f(\kappa)] \quad (22)$$

in the vicinity of the solution (21–20) and across the whole parameter space $(\kappa, \varepsilon_{dd}, \gamma)$. One finds that for $0 \leq \varepsilon_{dd} < 1$ the solution given by the transcendental equation (21) is always stable, in the sense that it corresponds to a global minimum of the energy functional. As ε_{dd} is increased and passes through unity the solution matches smoothly onto one that is only metastable, i.e. it is only a local minimum in the energy landscape, and the global minimum is then a (prolate) collapsed state with $\kappa \rightarrow 0$. At the same time as the turning of the stable into a metastable solution, a second branch of solutions appear at a smaller value of κ , which correspond to unstable saddle points that separate the local minimum of the metastable solution from the global minimum of the collapsed state at $\kappa = 0$ in the energy landscape. If one continues to increase ε_{dd} then one of two things happens, depending on the value of γ : if γ is less than a critical value, $\gamma < \gamma_{\text{crit}} = 5.1701$, then, as ε_{dd} increases, eventually the metastable and unstable solutions coalesce at $\varepsilon_{dd} = \varepsilon_{dd}^{\text{crit}}$, above which there are no solutions, not even metastable ones, and the energy landscape is just a continuous slope down towards a collapsed state with $\kappa = 0$. This critical value $\varepsilon_{dd}^{\text{crit}}$ as a function of γ is plotted in Figure 3. If, however, $\gamma > \gamma_{\text{crit}}$ then something rather surprising happens. As first remarked by Santos *et al* [5], when $\gamma > \gamma_{\text{crit}}$ there exists a solution metastable to scaling perturbations at a finite value of κ for all values of ε_{dd} , strictly speaking even for $\varepsilon_{dd} = \infty$. (Note, however, that our value for γ_{crit} disagrees with that of Ref. [5] but is that same as the one given in Ref. [9]).

For completeness we would like to mention that prima facie the transcendental equation (21) for $\varepsilon_{dd} > 1$ has solutions also for $\kappa > \gamma$. These come in pairs, one corresponding to a maximum and the other to a saddle point in the energy landscape. However, inspection reveals that these solutions have no physical relevance as for them the radius R_x of the condensate, Eq. (20), comes out imaginary.

C. Saturn-ring instability

An examination of the dipolar potential *outside* the condensate, that is seen, for example by a single test atom placed beyond the boundary $\rho^2/R_x^2 + z^2/R_z^2 = 1$, reveals a new type of possible instability. Like the lo-

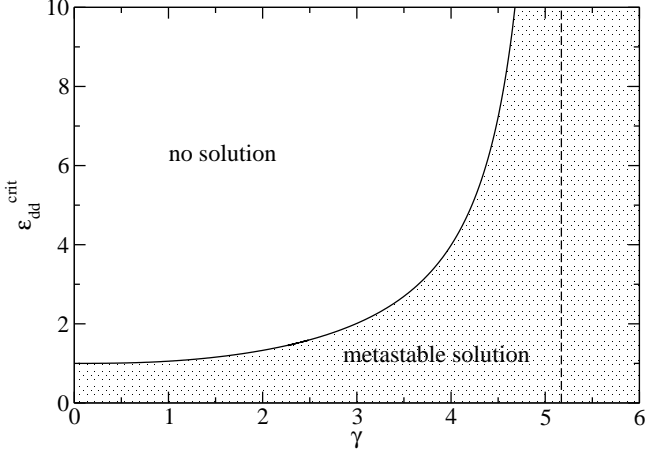


FIG. 3: The critical value of the dipolar coupling, $\varepsilon_{dd}^{\text{crit}}$, above which the condensate becomes strictly unstable—even the metastable state (local minimum in the energy landscape) no longer exists. However, above $\gamma_{\text{crit}} = 5.1701$, there is always a solution metastable to scaling deformations even for arbitrarily large ε_{dd} .

cal density perturbations, it also does not preserve the parabolic form of the density profile. It turns out that for $\varepsilon_{dd} > 1$ the potential seen by atoms just outside the condensate exhibits a local minimum, i.e. the sum of trap and dipole-dipole potentials is locally lower than the chemical potential, which causes atoms to tunnel out from the condensate and fill this dip in the potential. Such an effect is peculiar to condensates with induced dipole-dipole interactions because these are long-range and thus give rise to a potential even outside the condensate, whereas the potential due to *s*-wave scattering is short-range and thus zero outside the condensate. To investigate the dip in the outside potential we need to calculate $\Phi_{dd}(\mathbf{r})$ in Eq. (7) outside the condensate. Using relation (8) we can write the outside dipole-dipole potential in the same way as in Eq. (9), except that the term with δ_{ij} does not arise because $n(\mathbf{r})$ is obviously zero outside the condensate. Using the Green's function in prolate spheroidal coordinates we find for the potential (10) outside

$$\phi(\xi, \eta, \varphi) = \frac{R_z^2 - R_x^2}{2} \left[\int_1^{1/\sqrt{1-\kappa^2}} d\xi' \int_{-1}^1 d\eta' (\xi'^2 - \eta'^2) \times n(\xi', \eta') \sum_{\ell=0}^{\infty} (2\ell + 1) P_\ell(\eta) P_\ell(\eta') Q_\ell(\xi) P_\ell(\xi') \right],$$

where, as before, only $\ell = 0, 2, 4$ actually contribute to the sum. In the oblate case a similar formula applies, with just ξ and ξ' replaced by $i\xi$ and $i\xi'$ and the ξ' integration running from 0 to $1/\sqrt{\kappa^2 - 1}$. We obtain

$$\begin{aligned} \Phi_{dd}^{(\text{outside})}(\mathbf{r}) = & -\frac{3g\varepsilon_{dd}n_0\kappa^2}{4(1-\kappa^2)^{3/2}} \left\{ 6\xi(1-3\eta^2) \right. \\ & \left. + [9\xi^2\eta^2 - 3(\xi^2 + \eta^2) + 1] \ln \frac{\xi+1}{\xi-1} + 6\xi(1-3\eta^2) \right\} \end{aligned} \quad (23)$$

in the prolate case, and

$$\begin{aligned} \Phi_{dd}^{(\text{outside})}(\mathbf{r}) = & -\frac{3g\varepsilon_{dd}n_0\kappa^2}{4(\kappa^2-1)^{3/2}} \left\{ 6\xi(1-3\eta^2) \right. \\ & \left. + [9\xi^2\eta^2 - 3(\xi^2 - \eta^2) - 1] (\pi - 2 \arctan \xi) + 6\xi(1-3\eta^2) \right\} \end{aligned} \quad (24)$$

in the oblate case. These expressions can easily be converted back from prolate or oblate spheroidal coordinates (ξ, η) into Cartesian coordinates, as was described above, but we abstain from writing them down in Cartesian coordinates because there they are rather lengthy and unwieldy. Instead, we analyse the outside potential in spheroidal coordinates.

The outside potential \mathcal{V} is the sum of the trap potential and the dipole-dipole interaction potential $\Phi_{dd}^{(\text{outside})}(\mathbf{r})$. The trap potential is positive and monotonically rising from the center. The dipole-dipole interaction potential outside the condensate is a solution of the (homogeneous) Laplace equation, i.e. $\Phi_{dd}^{(\text{outside})}(\mathbf{r})$ is a harmonic function. Thus the Maximum Principle applies, and $\Phi_{dd}^{(\text{outside})}(\mathbf{r})$ must assume its maximum and minimum on the boundaries of the domain, either at infinity or on the surface of the condensate. At infinity the dipole-dipole potential vanishes, which means that at large distances the total outside potential is positive and dominated by the trap potential. To ascertain whether the outer potential \mathcal{V} has a local minimum one only needs to check whether the sum of trap and dipole-dipole potentials has a negative first derivative at the surface of the condensate in some outward direction. It is easy to see that local minima of \mathcal{V} can occur only for $\eta = 0$: at a local minimum of \mathcal{V} its first derivative with respect to ξ and η must vanish, but both the trap potential and the dipole-dipole potential are quadratic in η , so that the first derivative $\partial\mathcal{V}/\partial\eta$ is proportional to η and thus vanishes only for $\eta = 0$ unless it vanishes for all η . Therefore we only need to examine the derivative $\partial\mathcal{V}/\partial\xi$ at $\eta = 0$; we find

$$\frac{\partial}{\partial\xi} \left(\frac{\mathcal{V}}{\mu} \right) \Big|_{\xi=\xi_B, \eta=0} = \frac{2(1-\varepsilon_{dd})}{\xi_B\kappa^2[1-\varepsilon_{dd}f(\kappa)]} \quad (25)$$

where ξ_B is the value of the spheroidal variable ξ on the surface of the condensate, i.e. $\xi_B = 1/\sqrt{1-\kappa^2}$ for a prolate BEC and $\xi_B = 1/\sqrt{\kappa^2-1}$ for an oblate BEC. For oblate BECs the denominator in Eq (25) is always positive, and thus $\partial\mathcal{V}/\partial\xi$ is negative if and only if $\varepsilon_{dd} > 1$. For prolate BECs the denominator is always positive in the stable and metastable regions of Fig 1, and thus in these regions $\partial\mathcal{V}/\partial\xi$ is negative if and only if $\varepsilon_{dd} > 1$. Whenever $\partial\mathcal{V}/\partial\xi$ is negative on the condensate surface, a local minimum of the potential lies somewhere outside the surface. The fact that this happens at $\eta = 0$ means that the local dip in the potential occurs along a ring at $z = 0$ around the condensate, and the tunnelling out of atoms from the main condensate into the dip causes the condensate to take on a Saturn-like appearance, which then leads to further instability. Figure 4 gives an illustration of a typical potential, plotted as contours in the

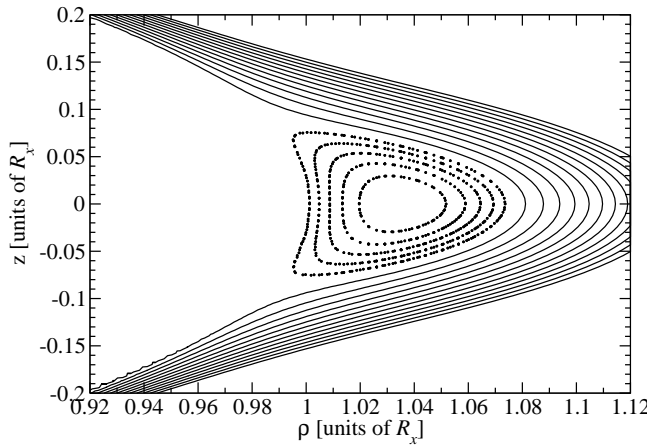


FIG. 4: Contour plot of the potential \mathcal{V} (in units of the chemical potential μ) outside a condensate with $\kappa = 2$ at $\varepsilon_{dd} = 1.5$. The closed contours drawn in dotted lines have $\mathcal{V}/\mu < 1$; the lowest in the middle is at $\mathcal{V}/\mu = 0.992$ and the difference to the next higher is roughly 0.0017. The cut off contours outside the condensate go from $\mathcal{V}/\mu = 1.002$ to 1.04 in steps of approximately 0.0034.

$\rho - z$ plane. The flat part to the left of the center is the constant chemical potential inside the condensate.

Finally, we would like to point out in this context that, aside from the purpose of assessing the stability of the condensate, it is useful in its own right to know the potential (23,24) outside a dipolar condensate for some applications. For example, in an array of dipolar BECs on a lattice the condensate at each lattice site can behave as a single mesoscopic spin [14]. In order to determine the spin-spin coupling between sites one needs to know the external potential generated by each condensate. At large distances $r = (\rho^2 + z^2)^{1/2}$ the dipole-dipole interaction potential is approximately:

$$\Phi_{dd}^{(\text{outside})}(\mathbf{r}) \simeq C_{dd} \frac{N}{4\pi r^3} \left[\left(1 - \frac{3z^2}{r^2} \right) + \frac{R_x^2 - R_z^2}{r^2} \left(\frac{9}{14} - \frac{45z^2}{7r^2} + \frac{15z^4}{2r^4} \right) + O\left(\frac{R_x, R_z}{r}\right)^4 \right] \quad (26)$$

which holds for both prolate and oblate condensates. It turns out that this asymptotic expression serves remarkably well even quite close to the condensate. We give a derivation from integration over thin ellipsoidal shells in Appendix B. Note that equation (26) says that to a first approximation, when seen from outside the dipolar condensate behaves like a single giant dipole of N -times the single-atom dipole magnitude. The higher multipoles depend on the shape of the BEC.

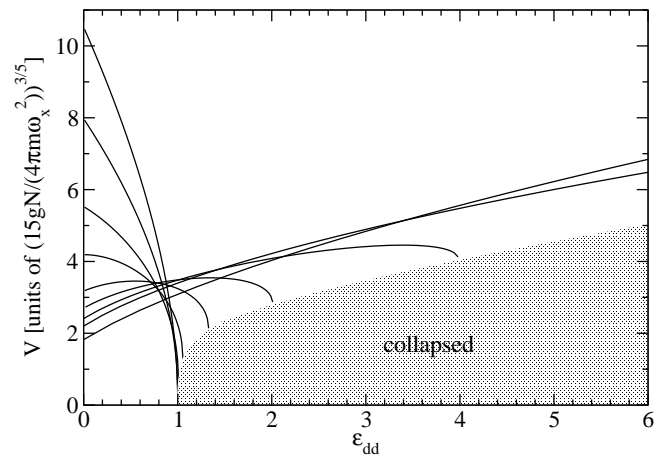


FIG. 5: The volume V of the condensate for traps with aspect ratios $\gamma = \{0.1, 0.2, 0.5, 1, 2, 3, 4, 5, 8\}$ as a function of the dipole-dipole coupling strength ε_{dd} . At $\varepsilon_{dd} = 0$, i.e. without dipole-dipole interactions, the volume is proportional to $\gamma^{-2/5}$, so that on the left edge of the graph higher volume corresponds to lower γ . That reverses with increasing ε_{dd} .

VI. ELECTROSTRICTION

The volume V of the spheroidal BEC can be expressed as

$$V = \frac{4\pi}{3} R_x^2 R_z = \frac{4\pi}{3} \frac{R_x^3}{\kappa} . \quad (27)$$

Substituting R_x from Eq. (20) we can write it as

$$V = \frac{4\pi}{3\kappa^{2/5}} \left[\frac{15gN}{4\pi m \omega_x^2} \right]^{3/5} \left[1 + \varepsilon_{dd} \left(\frac{3\kappa^2 f(\kappa)}{2(1-\kappa^2)} - 1 \right) \right]^{3/5} \quad (28)$$

and then we can use the transcendental equation (21) to eliminate κ in favor of γ and ε_{dd} . In Fig. 5 we plot V in units of $[15gN/(4\pi m \omega_x^2)]^{3/5}$ as a function of ε_{dd} for various trap aspect ratios γ . The figure shows that condensates in prolate traps and slightly oblate traps (with $\gamma < 1.6630$) get compressed by increasing dipolar interactions, while condensates in traps with aspect ratios above $\gamma_{\text{crit}} = 5.1701$ are being pulled apart as ε_{dd} rises. Between $\gamma = 1.6630$ and γ_{crit} is a range of trap aspect ratios for which the condensate is pulled apart at first but eventually compressed into collapse by higher values of the dipolar interaction strength. If, during an experiment, the condensate was imaged in the trap then the volume could be measured either directly from the radii, or by the central density which is inversely proportional to the volume, $V = (5/2)N/n_0$.

VII. RELEASE ENERGY

If the trap is turned off the condensate expands ballistically and the s -wave and dipole-dipole interaction energies are converted into kinetic energy, the so-called release energy, which can be measured in an experiment.

For the exact parabolic solution the release energy is given by

$$E_{\text{rel}} = 15gN^2[1 - \varepsilon_{\text{dd}}f(\kappa)]/(28\pi R_x^2 R_z). \quad (29)$$

The release energy can also be expressed in terms of the chemical potential (19) as $E_{\text{rel}} = (2/7)N\mu$, which is the standard expression for the Thomas-Fermi limit [2].

VIII. CONCLUSIONS

The long-range anisotropic nature of dipole-dipole interactions gives condensates composed of dipolar atoms or molecules novel properties compared to those with only short-range interactions. Furthermore, the dipole-dipole interactions can be controlled in both sign, magnitude and direction. We have shown that a simple inverted parabola remains an exact solution for the density-profile of a harmonically trapped dipolar BEC in the Thomas-Fermi limit by calculating the dipolar potential both inside and outside the condensate region. The parabolic solution is stable, in the strict Thomas-Fermi limit, only for $\varepsilon_{\text{dd}} < 1$. For $\varepsilon_{\text{dd}} > 1$ it is unstable either against scaling perturbations as seen in the energy functional, or against perturbations of different symmetry, such as phonons, or due to a local minimum appearing in the potential outside the condensate. The effect of the dipole-dipole interactions upon the BEC is to change both its aspect ratio and its volume. The manner of this electrostriction depends on the aspect ratio of the external trap; as a function of the strength of the dipole-dipole interactions (relative to the s -wave scattering) the volume of the BEC can either increase or decrease, or even initially increase and then decrease at higher values of the coupling.

Acknowledgments

It is a pleasure to thank Gabriel Barton for discussions. We would like to acknowledge financial support from the UK Engineering and Physical Sciences Research Council (D.O.D.) and from the European Union (S.G.), and we are indebted to the Royal Society for a University Research Fellowship (C.E.).

APPENDIX A: INTEGRATING OVER HOMOEOID SHELLS

Here we demonstrate how the potential (14) can be obtained by integrating over successive thin shells, a method that works even in the general case of an ellipsoid. The problem of the electrostatic/gravitational field within and outside a charged/massive ellipsoid is associated with some of the great names of nineteenth century mathematical physics. In his 1892 treatise on

statics, Routh [23] notes that Chasles, Dirichlet, Jacobi, and Poisson all made contributions. Rodrigues is credited with being the first to evaluate the potential of a solid ellipsoid of constant density, seemingly in 1815, and in 1833 Green [24] “treated the subject in a very general manner” giving solutions for various cases of inhomogeneous density, as in the current situation. Our derivation is adapted from Routh. Although we take a cylindrically symmetric density as input, in other respects the derivation holds for the general ellipsoidal case.

Consider an ellipsoidal surface $(x/R_x)^2 + (y/R_y)^2 + (z/R_z)^2 = 1$, having semi-axes (R_x, R_y, R_z) . A continuous family of concentric *similar* ellipsoids lying inside this outer surface can then be defined via the semi-axes (sR_x, sR_y, sR_z) , where $0 \leq s \leq 1$. Note that by similar we mean that this family all share the same aspect ratios among their semi-axes, but are consequently *not* confocal. A surface which is *confocal* to the original surface obeys $x^2/(R_x^2 + \lambda) + y^2/(R_y^2 + \lambda) + z^2/(R_z^2 + \lambda) = 1$, so that $\lambda = 0$ is obviously the original surface, and surfaces with $\lambda > 0$ lie outside the original. Considered in terms of the parameterization specified by s , the parabolic density profile can be written as $n = n_0(1 - s^2)$. Since the equi-density surfaces within the density profile are similar, when computing the integral (10) it makes sense to take as our basic volume element a thin “homoeoid” [23], defined as the shell bounded by two similar ellipsoidal surfaces, parameterized by s and $s+ds$, respectively. The volume of the thin homoeoid is $dV = 4\pi R_x R_y R_z s^2 ds$. When computing the potential at a point $\mathcal{P}(x, y, z)$ within a charged ellipsoid the contribution from the homoeoids interior to that point is of a different nature to that from those exterior to it, so we consider the two parts separately.

1. Potential ϕ^{in} due to ‘charge’ interior to \mathcal{P}

Let $d\phi$ denote the contribution to the total potential ϕ from a thin homoeoid shell. In this section we require the potential $d\phi^{\text{in}}$ *outside* a thin homoeoid, labelled by its inner surface s , whose ‘charge’ density is $n = n_0(1 - s^2)$. The equi-potential surfaces outside a charged thin homoeoid s are confocal ellipsoids [23]

$$\frac{x^2}{s^2 R_x^2 + \lambda} + \frac{y^2}{s^2 R_y^2 + \lambda} + \frac{z^2}{s^2 R_z^2 + \lambda} = 1 \quad (\text{A1})$$

In our analogy (in which the dielectric constant $\epsilon_0 = 1$) the ‘potential’ on a confocal surface λ outside a thin homoeoid labelled by s , of density n and volume dV is

$$d\phi_{\lambda}^{\text{in}}(s) = \frac{n dV}{8\pi} \int_{\lambda}^{\infty} \frac{du}{\sqrt{(s^2 R_x^2 + u)(s^2 R_y^2 + u)(s^2 R_z^2 + u)}}. \quad (\text{A2})$$

This potential is most easily obtained by noticing that the ‘charge’ distribution on the homoeoid is identical to

that of a solid ellipsoidal *conductor* with the same external dimensions and with the same total ‘charge’ (ndV) distributed over its surface. A homoeoid shell does not have uniform thickness, dh , being slightly thicker at the points furthest from the center

$$dh = \frac{s \, ds}{\sqrt{\frac{x^2}{R_x^4} + \frac{y^2}{R_y^4} + \frac{z^2}{R_z^4}}}. \quad (\text{A3})$$

If, rather than a shell of thickness dh we consider the ‘charge’ it contains to in fact be surface charge, of variable surface density $\omega(x, y, z)$, i.e. so that $\omega = nh$, we obtain exactly the same $\omega(x, y, z)$ as in the well-known problem of the charged ellipsoid conductor (see, e.g. [25]), and thus the resulting potentials are also the same.

Having established the potential due to a homoeoid shell we must integrate over all the shells s lying inside \mathcal{P} , which is located on the confocal surface λ . While \mathcal{P} is of course fixed in space, the surface λ passing through it is a different surface (i.e. different aspect ratio) for each homoeoid, i.e. $\lambda = \lambda(s)$, becoming at the last instant a similar surface to the final homoeoid (upon which \mathcal{P} itself sits). To simplify the algebra we put $\lambda = s^2\sigma$ in the equation for the ellipsoidal surface (A1). We see that if $s = 0$ then $\sigma = \infty$. We choose $s = \tilde{s}$ to describe the similar ellipsoidal surface upon which \mathcal{P} lies, and thus we have $\sigma = 0$ for $s = \tilde{s}$. To obtain the potential due to the charge interior to \mathcal{P} we must evaluate $\phi^{\text{in}} = \int_{s=0}^{\tilde{s}} d\phi_{\lambda}^{\text{in}}(s)$. Setting $u = s^2v$ in the integral (A2), we find

$$\phi^{\text{in}} = \frac{n_0 R_x R_y R_z}{2} \times \int_0^{\tilde{s}} ds (1 - s^2) s \int_{\sigma(s)}^{\infty} \frac{dv}{\sqrt{(R_x^2 + v)(R_y^2 + v)(R_z^2 + v)}} \quad (\text{A4})$$

which can be integrated by parts to give

$$\begin{aligned} \phi^{\text{in}} = & \frac{n_0 R_x R_y R_z}{2} \left\{ \left(\frac{\tilde{s}^2}{2} - \frac{\tilde{s}^4}{4} \right) \int_0^{\infty} \frac{dv}{\sqrt{(R_x^2 + v)(R_y^2 + v)(R_z^2 + v)}} \right. \\ & - \int_0^{\infty} \left[\frac{1}{2} \left(\frac{x^2}{R_x^2 + \sigma} + \frac{y^2}{R_y^2 + \sigma} + \frac{z^2}{R_z^2 + \sigma} \right) \right. \\ & \left. \left. - \frac{1}{4} \left(\frac{x^2}{R_x^2 + \sigma} + \frac{y^2}{R_y^2 + \sigma} + \frac{z^2}{R_z^2 + \sigma} \right)^2 \right] \right. \\ & \left. \times \frac{d\sigma}{\sqrt{(R_x^2 + \sigma)(R_y^2 + \sigma)(R_z^2 + \sigma)}} \right\}, \quad (\text{A5}) \end{aligned}$$

where in the second term we have used Leibniz’s formula for differentiating an integral and used Eq. (A1) to replace s^2 and s^4 .

2. Potential ϕ^{ex} due to ‘charge’ exterior to \mathcal{P}

The potential inside a homoeoid is much simpler to calculate since, just as in the case of the spherical shell, it is a constant, independent of position [26]. Returning to the solid ellipsoidal conductor model, the potential throughout a conductor is the same as on the surface defined by $\lambda = 0$. Thus

$$d\phi^{\text{ex}}(s) = \frac{n \, dV}{8\pi} \int_0^{\infty} \frac{du}{\sqrt{(s^2 R_x^2 + u)(s^2 R_y^2 + u)(s^2 R_z^2 + u)}}.$$

Note that because the lower limit of the integral is this time independent of s the ensuing treatment is simple. Integrating from the surface \tilde{s} , which includes \mathcal{P} , out the boundary $s = 1$, we require $\phi^{\text{ex}} = \int_{s=\tilde{s}}^1 d\phi^{\text{ex}}(s)$. Making once again the substitution $u = s^2v$ one immediately finds

$$\begin{aligned} \phi^{\text{ex}} = & \frac{n_0 R_x R_y R_z}{2} \left[\frac{1}{2} (1 - \tilde{s}^2) - \frac{1}{4} (1 - \tilde{s}^4) \right] \\ & \times \int_0^{\infty} \frac{dv}{\sqrt{(R_x^2 + v)(R_y^2 + v)(R_z^2 + v)}}. \quad (\text{A6}) \end{aligned}$$

Combining Eqs. A5 and A6 we see that the parameter \tilde{s} drops from the sum $\phi^{\text{tot}} = \phi^{\text{in}} + \phi^{\text{ex}}$. In the general ellipsoidal case the remaining integrals in ϕ^{tot} can be expressed in terms of elliptic integrals. In the spheroidal case ($R_x = R_y$) they can be written in terms of more elementary functions. There are two cases to distinguish, depending upon whether the density profile is prolate (a cigar), $R_z > R_x$, or oblate (a pancake), $R_x > R_z$. If we define

$$\begin{aligned} \mathcal{J}(a, c) \equiv & \int_0^{\infty} \frac{dv}{(R_x^2 + v) \sqrt{(R_z^2 + v)}} \\ = & \begin{cases} \frac{1}{\sqrt{R_z^2 - R_x^2}} \ln \left(\frac{1 + \sqrt{1 - R_x^2/R_z^2}}{1 - \sqrt{1 - R_x^2/R_z^2}} \right) & \text{prolate} \\ \frac{2}{\sqrt{R_x^2 - R_z^2}} \arctan \left(\sqrt{R_x^2/R_z^2 - 1} \right) & \text{oblate} \end{cases} \end{aligned}$$

then the total potential at \mathcal{P} is most compactly expressed as

$$\begin{aligned} \phi^{\text{tot}} = & \frac{n_0 R_x^2 R_z}{2} \left(\frac{\mathcal{J}}{4} + \frac{\rho^2}{2} \frac{\partial \mathcal{J}}{\partial (R_x^2)} + z^2 \frac{\partial \mathcal{J}}{\partial (R_z^2)} \right. \\ & \left. + \frac{\rho^4}{8} \frac{\partial^2 \mathcal{J}}{\partial (R_x^2)^2} + \frac{z^4}{3} \frac{\partial^2 \mathcal{J}}{\partial (R_z^2)^2} + \rho^2 z^2 \frac{\partial^2 \mathcal{J}}{\partial (R_x^2) \partial (R_z^2)} \right) \quad (\text{A7}) \end{aligned}$$

and is identical to the Green’s function result (14). The relationship between the function Ξ defined in the Green’s function approach and \mathcal{J} defined here is simply $\mathcal{J} = \Xi/R_z$.

APPENDIX B: THE POTENTIAL OUTSIDE THE CONDENSATE

The calculation of the potential at a point \mathcal{P} outside the boundary of the condensate follows very similar lines to that presented above for a point inside. The main difference is that one no longer has to consider ‘charge’ located exterior to \mathcal{P} . The result is identical to Eq. (A7) except that the integral \mathcal{J} is now given by

$$\begin{aligned} \mathcal{J}(a, c, \lambda) &\equiv \int_{\lambda}^{\infty} \frac{dv}{(R_x^2 + v)\sqrt{(R_z^2 + v)}} \\ &= \begin{cases} \frac{1}{\sqrt{R_z^2 - R_a^2}} \ln \left(\frac{\sqrt{\lambda + R_z^2} + \sqrt{R_z^2 - R_x^2}}{\sqrt{\lambda + R_z^2} - \sqrt{R_z^2 - R_x^2}} \right) & \text{pro.} \\ \frac{2}{\sqrt{R_x^2 - R_z^2}} \arctan \left(\sqrt{\frac{R_x^2 - R_z^2}{\lambda + R_z^2}} \right) & \text{ob.} \end{cases} \end{aligned}$$

where λ parameterizes an ellipse, confocal to the outer-boundary of the condensate, upon which the point \mathcal{P} sits, and so obeys the quadratic equation $\rho^2/(R_x^2 + \lambda) + z^2/(R_z^2 + \lambda) = 1$. When solving for λ one should take the positive solution

$$\lambda = \frac{\rho^2 - R_x^2 + z^2 - R_z^2}{2} + \frac{\sqrt{(\rho^2 - R_x^2 + z^2 - R_z^2)^2 + 4(\rho^2 R_z^2 + z^2 R_x^2 - R_x^2 R_z^2)}}{2}.$$

Note that expressing the solution for the potential ϕ in the form (A7) requires that when taking the derivatives with respect to R_x and R_z then λ is to be treated as a constant and is *not* to be differentiated. On the other hand, when going on to calculate the dipolar potential outside the BEC, $\Phi_{dd} = -C_{dd} \hat{e}_i \hat{e}_j \nabla_i \nabla_j \phi(\mathbf{r})$, then λ is to be treated as a function of (ρ, z) , and should be differentiated. This makes the exact expression for Φ_{dd} outside the condensate complicated. However, in the limit $\rho \gg R_x, z \gg R_z$, one may use the asymptotic result

$$\phi^{\text{outside}} \sim \frac{N}{8\pi} \frac{(R_x^2 - R_z^2)(\rho^2 - 2z^2) + 14(\rho^2 + z^2)^2}{7(\rho^2 + z^2)^{5/2}} \quad (\text{B1})$$

which turns out in practice to be remarkably accurate, even right up to the condensate surface providing the condensate is not too aspherical (in which case the next terms in the multipole expansion should be included.)

[1] W. Ketterle, D.S. Durfee and D.M. Stamper-Kurn, Proc. Int. Sch. Phys. ‘Enrico Fermi’, Course CXL, edited by M. Inguscio, S. Stringari and C.E. Wieman (IOS Press, Amsterdam, 1999).

[2] F. Dalfovo, S. Giorgini, L.P. Pitaevskii and S. Stringari, Rev. Mod. Phys. **71**, 463 (1999).

[3] L.P. Pitaevskii, Sov. Phys. JETP, **13**, 451 (1961); E.P. Gross, Nuovo Cimento **20**, 454 (1961); J. Math. Phys. **4**, 195 (1963).

[4] K. Góral, K. Rzżewski, and T. Pfau, Phys. Rev. A **61**, 051601 (2000); J.-P. Martikainen, M. Mackie, and K.-A. Suominen, Phys. Rev. A **64**, 037601 (2001).

[5] L. Santos, G.V. Shlyapnikov, P. Zoller, and M. Lewenstein, Phys. Rev. Lett. **85**, 1791 (2000).

[6] P.M. Lushnikov, Phys. Rev. A **66**, 051601(R) (2002).

[7] S. Giovanazzi, D. O’Dell, and G. Kurizki, Phys. Rev. Lett. **88**, 130402 (2002).

[8] K. Góral, L. Santos, and M. Lewenstein, Phys. Rev. Lett. **88**, 170406 (2002).

[9] S. Yi and L. You, Phys. Rev. A **63**, 053607 (2001).

[10] K. Góral and L. Santos, Phys. Rev. A **66**, 023613 (2002).

[11] D.H.J. O’Dell, S. Giovanazzi and G. Kurizki, Phys. Rev. Lett. **90**, 110402 (2003).

[12] L. Santos, G.V. Shlyapnikov, and M. Lewenstein, Phys. Rev. Lett. **90**, 250403 (2003).

[13] D.H.J. O’Dell, S. Giovanazzi and C. Eberlein, cond-mat/0308096.

[14] K. Gross, C.P. Search, H. Pu, W. Zhang and P. Meystre, Phys. Rev. A **66**, 033603 (2002).

[15] M. Marinescu and L. You, Phys. Rev. Lett. **81**, 4596 (1998).

[16] S. Yi and L. You, Phys. Rev. A **61**, 041604 (2000).

[17] S. Giovanazzi, A. Görlitz and T. Pfau, Phys. Rev. Lett. **89**, 130401 (2002).

[18] S. Yi and L. You, Phys. Rev. A **67**, 045601 (2003).

[19] D. O’Dell, S. Giovanazzi, G. Kurizki and V.M. Akulin, Phys. Rev. Lett. **84**, 5687 (2000); S. Giovanazzi, D. O’Dell, and G. Kurizki, Phys. Rev. A **63**, 031603 (2001); S. Giovanazzi, D. O’Dell, and G. Kurizki, J. Phys. B **34**, 4757 (2001); S. Giovanazzi, G. Kurizki, I. E. Mazets, and S. Stringari, Europhys. Lett. **56**, 1 (2001); G. Kurizki, S. Giovanazzi, D. O’Dell and A.I. Artemiev in *Dynamics and Thermodynamics of Systems with Long-Range Interactions*, edited by T. Dauxois *et al.*, Lecture Notes in Physics Vol. 602 (Springer, Berlin, 2002).

[20] P. M. Morse and H. Feshbach, *Methods of Theoretical Physics*, Vol. II, §10.3 (McGraw-Hill, New York 1953).

[21] Note that eq. (10.3.63) in [20] is misprinted and should be divided by 2.

[22] S. Giovanazzi, A. Görlitz and T. Pfau, J. Opt. B **5** (2003).

[23] E.J. Routh, *A Treatise in Analytical statics*, Vol. II (Cambridge, 1892).

[24] G. Green, *On the Determination of Exterior and Interior Attractions of Ellipsoids of Variable Densities* (Cambridge Philosophical Society, read 6 May 1833, printed in the Transactions, Vol V, Part III, 1835).

- [25] J.A. Stratton, *Electromagnetic Theory* (McGraw-Hill, New York, 1941), p 209.
- [26] A.M. Portis, *Electromagnetic Fields* (Wiley, New York, 1978), p 44.